JACS
JOURNAL OF THE AMERICAN CHEMICAL SOCIETY
Communication
pubs.acs.org/JACS

Three-State Near-Infrared Electrochromism at the Molecular Scale

Bin-Bin Cui, Yu-Wu Zhong,* and Jiannian Yao

Beijing National Laboratory for Molecular Sciences, CAS Key Laboratory of Photochemistry, Institute of Chemistry, Chinese Academy of Sciences, Beijing 100190, People's Republic of China

Supporting Information

ABSTRACT: Self-assembled monolayer films of a cyclometalated ruthenium complex with a redox-active amine substituent and three carboxylic acid groups have been prepared on ITO electrode surfaces. The obtained thin films show three-state electrochromic switching with low electrochemical potential inputs and high near-infrared absorbance outputs. Thanks to the long retention time of each oxidation states, these films have been used to demonstrate surface-confined flip-flop memory functions with high ON/OFF ratios at the molecular scale.

Molecular materials that can respond to external stimulus hold great promise for miniaturized devices with switching and memory functions.[1] For eventual practical applications, the confinement of solution-phase demonstrations to solid support is essential.[2] The molecular materials can be deposited in the form of monolayer,[3] multilayer,[4] or polymeric thin films.[5] Smart surfaces with monolayer of molecular materials are particularly appealing in achieving high information density with the smallest device size. However, it is extremely difficult to realize a high ON/OFF ratio in monolayer molecular devices, due to the low output signal at the molecular scale and the severe interference of the background noises.[3] In addition, most reported surface-confined molecular switches are bistable, and they are useful for the construction of binary logic gates. To further increase the information capacity, it would be charming to develop tristable materials and devices. Up to date, thin films with three-state switching are very rare.[6]

We present herein a monolayer-based molecular switch that can perform three-state switching with electrochemical inputs and near-infrared (NIR) optical outputs, namely NIR electrochromism[7] at the molecular scale. The use of electrical inputs is compatible with existing electronic technologies. NIR absorption signals as the outputs have the advantages of being low energy, nondestructive, and low interference with substrates.[8] In addition, the common optic fiber telecommunication wavelengths are in the NIR region. NIR electrochromic materials are useful as variable optical attenuators (VOA) in optical telecommunications.[9] NIR electrochromism on the basis of polymeric thin films have been demonstrated.[5,9,10] However, NIR electrochromism based on the monolayer films has not been possible to date.

The molecule used for forming the monolayer film is the ruthenium complex **1**(PF_6) (Figure 1), where a Ru−C bond is present with a redox-active dianisylamino substituent on the *para* position of the Ru−C bond. Three carboxylic groups are installed on the terpyridine ligand as the anchoring groups for film formation on ITO surfaces. The use of multidentate carboxylic ligands for the formation of stable films has been well established.[11] Previous studies showed that the strong ruthenium-amine electronic coupling of related compounds with no carboxylic groups resulted in two stepwise redox waves with a potential separation over 400 mV.[12] As a result, three distinct redox states are available and each state display significantly different NIR absorption spectrum in solution.

Complex **1**(PF_6) was synthesized from the known methyl ester precursor **2**(PF_6)[12b] as depicted in the Supporting Information, SI. The self-assembled monolayer (SAM) was prepared by immersing the freshly cleaned ITO glass electrode in 0.1 mM of **1**(PF_6) in MeOH for appropriate time, followed by washing with copious MeOH and CH_2Cl_2 and sonication in clean CH_2Cl_2 for 1 min. The thus-obtained thin film shows two redox waves at +0.23 and +0.65 V vs Ag/AgCl (Figure 2a). The film has good electrochemical stability. The shape of the cyclic voltammogram (CV) is essentially retained after 500 potential cycling between 0 and +0.8 V. Each redox couple has a peak-to-peak potential separation of 40 mV. Both anodic and cathodic currents are linearly dependent on the scan rate (Figure S1, SI), characteristic of surface-confined redox behavior. The 40 mV peak-to-peak potential separation is partially caused by the charge repulsion between neighboring metal complexes. The methyl ester **2**(PF_6) did not bind to ITO at all (see the magenta curve in Figure 2a), indicating that the interaction between the carboxylic group and ITO is key to the formation of the SAM.

Figure 2b shows the plot of the surface coverage (Γ, determined by the charge under the electrochemical waves) versus the immersing time consumed for the preparation of the SAM. Around 20 h are needed to reach saturation with a maximum Γ of 2.4×10^{-10} mol/cm^2. This coverage is higher with the previously reported SAMs of a hexacoordinated osmium polypyridyl complex ($\Gamma \sim 1 \times 10^{-10}$ mol/cm^2).[13] One possible reason is that complex **1**(PF_6) has a very short linker, which tends to give a higher coverage. Indeed, SAMs of bis-tridentate ruthenium complexes up to 4×10^{-10} mol/cm^2 coverage has been reported recently.[14] Another possibility is that neighboring molecules **1**(PF_6) are densely packed due to weak intermolecular interaction, e.g., by hydrogen bonding from the free carboxylic groups. The above-mentioned peak-to-peak potential separation is a result of such dense packing.

The water contact angle of the **1**(PF_6)/ITO SAM is 35.5°, compared to 55.9° for the bare ITO glass (Figure S2). This

Received: January 18, 2015
Published: March 16, 2015

DOI: 10.1021/jacs.5b00586
J. Am. Chem. Soc. 2015, 137, 4058−4061

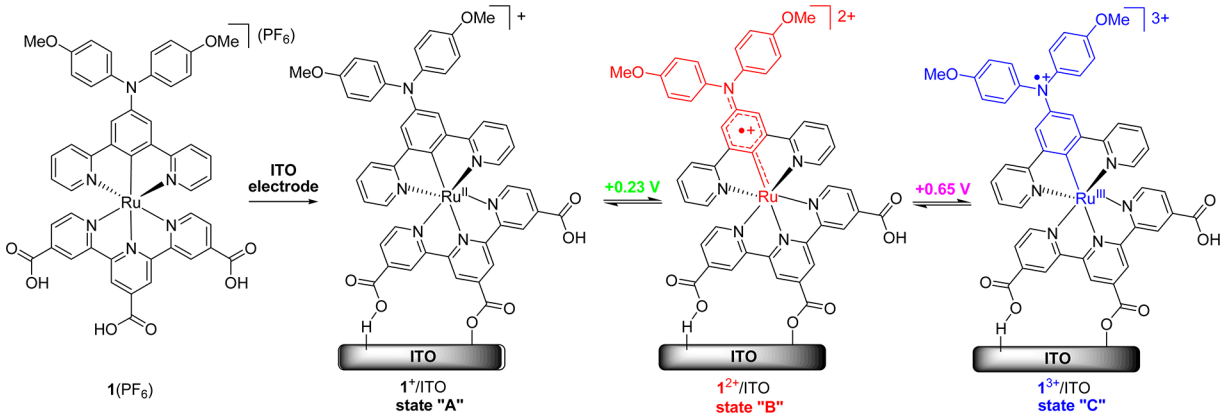

Figure 1. Schematic presentation of the preparation and electrochemically addressable three-redox-state switching of $\mathbf{1}^{n+}$/ITO SAM.

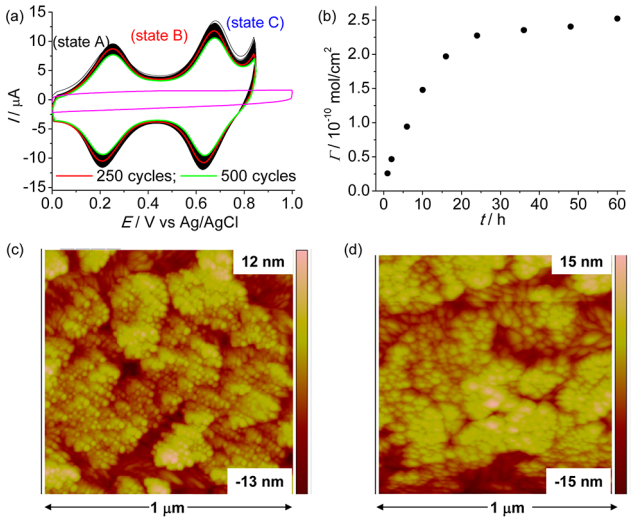

Figure 2. (a) Anodic CV of the $\mathbf{1}^{n+}$/ITO SAM ($\Gamma = 2.4 \times 10^{-10}$ mol/cm^2) at 50 mV/s in 0.1 M Bu_4NClO_4/CH_2Cl_2. The magenta curve is the CV of ITO after immersing in solution of methyl ester $\mathbf{2}(PF_6)$. (b) The plot of the surface coverage of the SAM versus the immersion time of the ITO electrode in 0.1 mM $\mathbf{1}(PF_6)$/MeOH during the preparation of the SAM. (c,d) AFM height images of the bare ITO glass and the $\mathbf{1}(PF_6)$/ITO SAM (1 μm × 1 μm in size), respectively.

indicates that the ITO surface becomes more hydrophilic after functionalization with $\mathbf{1}(PF_6)$, possibly caused by the presence of free carboxylic group of the ruthenium complex. Figure 2c,d shows the surface morphology of the bare ITO glass and the $\mathbf{1}(PF_6)$/ITO SAM measured by atomic force microscopy (AFM), respectively. They have similar surface topography with a mean roughness (rms) of 3.0 and 3.4 nm, respectively. No apparent aggregates are observed in Figure 2d. This suggests a rather homogeneous adsorption of the molecules on the electrode surface. Considering the good electrochemical stability and a surface coverage in the order of 10^{-10} mol/cm^2 of these films, the possibility of forming multilayer films is low.

The binding mode of carboxylic group with ITO glass is believed complex. Weak electrostatic and hydrogen bonding interaction and covalent bonding between the carboxylate and the metal ion defect sites of ITO are possible.[15] Powedered oxides were previously used as the substitute of ITO for FTIR measurements to probe the interaction between molecules and substrates.[15] After adsorbed on In_2O_3 powders, the carbonyl signal of $\mathbf{1}(PF_6)$ at 1732 cm^{-1} disappeared, with the appearance of a new peak at 1535 cm^{-1} (Figure S3). The latter peak is possibly from the carbonyl vibration of the carboxylates of $\mathbf{1}(PF_6)$ on In_2O_3 surfaces. Considering a relatively high coverage of the $\mathbf{1}(PF_6)$/ITO SAM, most molecules are believed to stand upright with a bidentate binding mode, as shown by the schematic representation in Figure 1. The X-ray photoelectron spectrum (XPS) of the film evidence the Ru 3d5 signal at 280.6 eV (Figure S4 and Table S1). However, the Ru/N integration ratio (0.06/2.24) is much lower with respect to the theoretical value (1/6).

The above film displays two well-defined redox couples at low potentials with a wide potential separation. As a result, three distinct redox states (state "A", "B", and "C" in Figures 1 and 2a) can be distinguished. In state "A", the amine is neutral and the ruthenium ion is in the +2 oxidation state. In state "B", one free radical spin is delocalized across the amine-ruthenium array. The amine unit is in the form of an aminium radical cation and the ruthenium ion has +3 oxidation state in state "C".[12]

Spectroelectrochemical measurements were performed on the $\mathbf{1}^{n+}$/ITO SAM to characterize the absorption spectra in different states (Figure 3a,b). Surprisingly, these films exhibit rather high NIR absorbance signal even at the monolayer scale. In state "A", the SAM has an absorbance of 0.0080 at 560 nm ($A_{560@A} = 0.0080$), which is due to the metal-to-ligand charge transfer (MLCT) transition of $\mathbf{1}^+$. The same order of magnitude of MLCT absorbance has previously been reported for a SAM based on a polypyridyl osmium complex.[16] In state "B", the MLCT absorption decreased a little, and an intense intervalence charge transfer band of $\mathbf{1}^{2+}$ appeared at 1020 nm ($A_{1020@B} = 0.0057$), which was very weak in state "A" ($A_{1020@A} = 0.0015$). In state "C", the $A_{1020@C}$ value decreased to 0.0012, and an intense $N^{\bullet+}$-localized transition at 700 nm appeared with the A_{700} value increased from 0.0005 ($A_{700@B}$) to 0.010 ($A_{700@C}$).

The optical memory effect (the ability to retain the absorbance value after the applied potential is switched off) was tested for the above SAM to verify its applicability in information storage (Figure 3c). In state "A", the SAM is very stable. The absorbance at 1020 nm kept constantly at a very low value after the potential at +0.01 V was released ($A_{1020@A} = 0.001$; 100 min measured). The retention time at state "B" is also very long even at the form of monolayer. When the potential at +0.50 V was turned off, the absorbance at 1020 nm decreased 22% from +0.007 to +0.0055 after 2 h. The retention

DOI: 10.1021/jacs.5b00586
J. Am. Chem. Soc. 2015, 137, 4058−4061

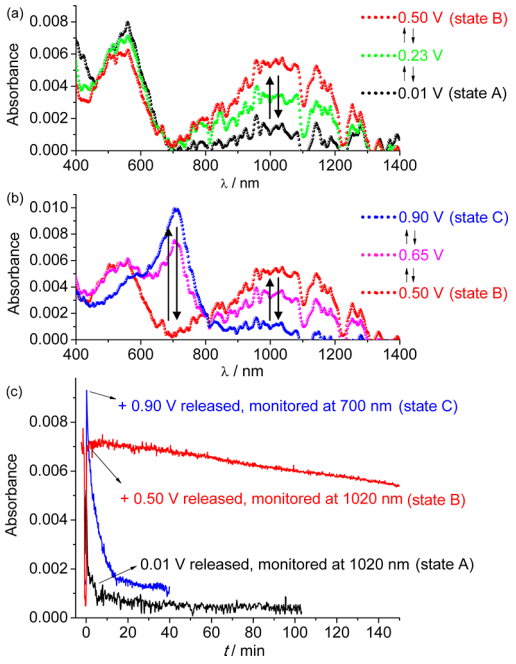

Figure 3. (a,b) Absorption spectral changes of the $\mathbf{1}^{n+}$/ITO SAM (Γ = 2.4 × 10^{-10} mol/cm^2) during spectroelectrochemical measurements. The applied potentials are referenced vs Ag/AgCl. (c) Retention time measurement of the $\mathbf{1}^{n+}$/ITO SAM at three states.

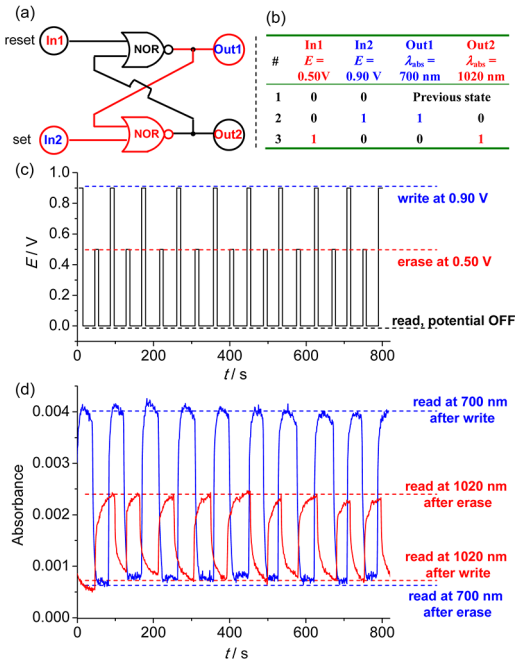

Figure 4. (a,b) Logic circuit and truth table of the set/reset flip-flop logic. (c,d) Switching of the input potentials (vs Ag/AgCl) and output absorbance at 700 and 1020 nm of $\mathbf{1}^{n+}$/ITO SAM (Γ = 1.0 × 10^{-10} mol/cm^2).

time at state "C" is around 10 min, which is good enough for their uses as volatile memory.

Figure S5 shows the results of the repetitive three-state electrochromic switching of the $\mathbf{1}^{n+}$/ITO SAM by four-potential-step chronoamperometry (one cycle: +0.01 → +0.50 → +0.90 → +0.50 → +0.01 V). The absorbance at 1020 nm is high at +0.50 V and experiences two switching processes within one potential cycle. On the other hand, the absorbance at 700 nm is high at +0.90 V and only experiences one switching process within one potential cycle. This three-state switching is fully reproducible after numerous potential cycling.

Alternatively, two-state switching can be performed by double-potential-step chronoamperometry. Figure S6 shows the absorbance change at 1020 nm between state "B" and "C" during the 100 potential cycles (+0.50 → +0.90 → +0.50 V) tested. The absolute absorbance values fluctuate slightly. However, the difference between $A_{1020@B}$ and $A_{1020@C}$ remains essentially unchanged. This attests to the good stability of the film during the electrochemical switching.

The long retention time of the $\mathbf{1}^{n+}$/ITO SAM makes it appealing for memory applications. Taking the electrochemical potential at +0.50 and +0.90 V as the input 1 and 2 signals (In1 and In2) and the absorbance at 700 and 1020 nm as the output 1 and 2 signals (Out1 and Out2), the $\mathbf{1}^{n+}$/ITO SAM can be considered as a surface-confined sequential molecular logic with set/reset flip-flop memory functions (Figure 4).[17] When In2 is applied, the Out1 signal is high and the output string is 10. On the other hand, when In1 is applied, the Out2 signal is high. Note that only one input signal can be applied at the same time. When the input string is 00 (namely, no potential is applied), the output signal is dependent on the previously memorized state.

Figure 4c,d shows the input and output signal changes of the above memory device during the repetitive "write-read-erase-read" cycles. The device was first subjected to a "write" process by applying a potential at +0.90 V for 10 s. The potential was then switched off, followed by a "read" process by either Out1 or Out2 for 30 s. The Out1 signal is high ($A_{700@write}$ = 0.004) and the Out2 signal is low ($A_{1020@write}$ = 0.0005) at this stage. The device was then subjected to an "erase" process by applying a potential at +0.50 V for another 10 s, followed by a similar "read" process for 30 s. The Out1 signal is now low ($A_{700@erase}$ = 0.0006) and the Out2 signal is turned high ($A_{1020@erase}$ = 0.0024). The difference between the high and low absorbance (ΔA) is 0.0034 and 0.0019 for Out1 and Out2, respectively. The ON/OFF ratio (the ratio between the high and low absorbance) is 6.7 and 4.8 for Out1 and Out2, respectively. This performance is retained after numerous "write−read−erase−read" cycles. These ON/OFF ratios are in fact rather high compared to the state-of-the-art monolayer switches with visible optical outputs. For instance, Veciana and Rovira and co-workers reported the bistable SAM switches on the basis of chloro-substituted triphenylmethly radicals with an ON/OFF ratio around 3 for the absorption signal at 515 nm.[3c] In addition, van der Boom and co-workers reported the monolayer logic gate on the basis of polypyridyl osmium complexes with a similar ON/OFF ratio around 3−4 for the absorption signal at 516 nm.[18] However, electrochromic ON/OFF ratios for NIR signals based on monolayer films have not been documented to date.

In conclusion, we have demonstrated the use of a self-assembled monolayer of a ruthenium complex for the three-state NIR electrochromic switching. The use of multidentate carboxylic ligands is beneficial for the formation of stable film with high surface coverage and good switching reversibility. The obtained monolayer film exhibits intense NIR absorbance and long optical retention time at each readily accessible oxidation states. This film provides an excellent molecular platform for the construction of surface-confined flip-flop

DOI: 10.1021/jacs.5b00586
J. Am. Chem. Soc. 2015, 137, 4058−4061

systems with high ON/OFF ratios (in terms of monolayer switches). It is very attractive for the preparation of NIR electrochromic and memory devices at the molecular scale.

■ ASSOCIATED CONTENT

Supporting Information

Synthesis and characterization of $\mathbf{1}(PF_6)$, preparation, characterization, and NIR electrochromic switching of $\mathbf{1}(PF_6)$/ITO SAM. This material is available free of charge via the Internet at http://pubs.acs.org.

■ AUTHOR INFORMATION

Corresponding Author

*zhongyuwu@iccas.ac.cn

Notes

The authors declare no competing financial interest.

■ ACKNOWLEDGMENTS

We thank the National Natural Science Foundation of China (Grants 91227104, 21271176, 21472196, and 21221002), the National Basic Research 973 program of China (Grant 2011CB932301), the Ministry of Science and Technology of China (Grant 2012YQ120060), and the Strategic Priority Research Program of the Chinese Academy of Sciences (Grant XDB 12010400) for funding support.

■ REFERENCES

(1) (a) Meng, F.; Hervault, Y.-M.; Shao, Q.; Hu, B.; Norel, L.; Rigaut, S.; Chen, X. *Nat. Commm.* **2014**, *5*, 3023. (b) Pochorovski, I.; Diederich, F. *Acc. Chem. Res.* **2014**, *47*, 2096. (c) Amelia, M.; Zou, L.; Credi, A. *Coord. Chem. Rev.* **2010**, *254*, 2267. (d) Audebert, P.; Miomandre, F. *Chem. Sci.* **2013**, *4*, 575.

(2) (a) Pischel, U. *Angew. Chem., Int. Ed.* **2010**, *49*, 1356. (b) Mas-Torrent, M.; Rovira, C.; Veciana, J. *Adv. Mater.* **2013**, *25*, 462. (c) de Ruiter, G.; Lahav, M.; van der Boom, M. E. *Acc. Chem. Res.* **2014**, *47*, 3407. (d) Winter, A.; Hoeppener, S.; Newkome, G. R.; Schubert, U. S. *Adv. Mater.* **2011**, *23*, 3484.

(3) (a) Liu, Z.; Yasseri, A. A.; Lindsey, J. S.; Bocian, D. F. *Science* **2003**, *302*, 1543. (b) Sortino, S.; Petralia, S.; Conoci, S.; Bella, S. D. *J. Am. Chem. Soc.* **2003**, *125*, 1122. (c) Simao, C.; Mas-Torrent, M.; Crivillers, N.; Lloveras, V.; Artes, J. M.; Gorostiza, P.; Veciana, J.; Rovira, C. *Nat. Chem.* **2011**, *3*, 359. (d) Terada, K.; Kanaizuka, K.; Iyer, V. M.; Sannodo, M.; Saito, S.; Kobayashi, K.; Haga, M.-a. *Angew. Chem., Int. Ed.* **2011**, *50*, 6287. (e) Yamanoi, Y.; Nishihara, H. *Chem. Commun.* **2007**, 3983.

(4) (a) Maier, A.; Rabindranath, A. R.; Tieke, B. *Adv. Mater.* **2009**, *21*, 959. (b) Sakamoto, R.; Katagiri, S.; Maeda, H.; Nishihara, H. *Coord. Chem. Rev.* **2013**, *257*, 1493. (c) Poppenberg, J.; Richter, S.; Traulsen, C. H.-H.; Darlatt, E.; Baytekin, B.; Heinrich, T.; Deutinger, P. M.; Huth, K.; Unger, W. E. S.; Schalley, C. A. *Chem. Sci.* **2013**, *4*, 3131.

(5) (a) Chen, X.-Y.; Yang, X.; Holliday, B. J. *J. Am. Chem. Soc.* **2008**, *130*, 1546. (b) Powell, A. P.; Bielawski, C. W.; Cowley, A. H. *J. Am. Chem. Soc.* **2010**, *132*, 10184. (c) Yao, C.-J.; Zhong, Y.-W.; Nie, H.-J.; Abruña, H. D.; Yao, J. *J. Am. Chem. Soc.* **2011**, *133*, 20720. (d) Cui, B.-B.; Yao, C.-J.; Yao, J.; Zhong, Y.-W. *Chem. Sci.* **2014**, *5*, 932.

(6) (a) de Ruiter, G.; Motiei, L.; Choudhury, J.; Oded, N.; van der Boom, M. E. *Angew. Chem., Int. Ed.* **2010**, *49*, 4780. (b) Simao, C.; Mas-torrent, M.; Casado-Montenegro, J.; Oton, F.; Veciana, J.; Rovira, C. *J. Am. Chem. Soc.* **2011**, *133*, 13256.

(7) (a) Mortimer, R. J. *Chem. Soc. Rev.* **1997**, *26*, 147. (b) Beaujuge, P. M.; Reynolds, J. R. *Chem. Rev.* **2010**, *110*, 268.

(8) (a) Qian, G.; Wang, Z. Y. *Chem.—Asian J.* **2010**, *5*, 1006. (b) Fablan, J.; Nakazumi, H.; Matsuoka, M. *Chem. Rev.* **1992**, *92*, 1197. (c) Kaim, W. *Coord. Chem. Rev.* **2011**, *255*, 2503.

(9) Wang, S.; Li, X.; Xun, S.; Wan, X.; Wang, Z. Y. *Macromolecules* **2006**, *39*, 7502.

(10) (a) Garcíña-Canadas, J.; Meacham, A. P.; Peter, L. M.; Ward, M. D. *Angew. Chem., Int. Ed.* **2003**, *42*, 3011. (b) Chandrasekhar, P.; Zay, B. J.; Birur, G. C.; Rawal, S.; Pierson, E. A.; Kauder, L.; Swanson, T. *Adv. Funct. Mater.* **2002**, *12*, 95. (c) Yen, H.-J.; Lin, H.-Y.; Liou, G.-S. *Chem. Mater.* **2011**, *23*, 1874.

(11) (a) Argazzi, R.; Iha, N. Y. M.; Zabri, H.; Odobel, F.; Bignozzi, C. A. *Coord. Chem. Rev.* **2004**, *248*, 1299. (b) Matsuo, Y.; Kanaizuka, K.; Matsuo, K.; Zhong, Y.-W.; Nakae, T.; Nakamura, E. *J. Am. Chem. Soc.* **2008**, *130*, 5016.

(12) (a) Yao, C.-J.; Zheng, R.-H.; Shi, Q.; Zhong, Y.-W.; Yao, J. *Chem. Commun.* **2012**, *48*, 568. (b) Yao, C.-J.; Nie, H.-J.; Yang, W.-W.; Shao, J.-Y.; Yao, J.; Zhong, Y.-W. *Chem.—Eur. J.* **2014**, *20*, 17466.

(13) (a) Acevedo, D.; Bretz, R. L.; Tirado, J. D.; Abruna, H. D. *Langmuir* **1994**, *10*, 1300. (b) Walsh, D. A.; Keyes, T. E.; Hogan, C. F.; Forster, R. J. *J. Phys. Chem. B* **2001**, *105*, 2792.

(14) Liatard, S.; Chauvin, J.; Balestro, F.; Jouvenot, D.; Loiseau, F.; Deronzier, A. *Langmuir* **2012**, *28*, 10916.

(15) (a) Meyer, T. J.; Meyer, G. J.; Pfennig, B. W.; Schoonover, J. R.; Timpson, C. J.; Wall, J. F.; Kobusch, C.; Chen, X.; Peek, B. M.; Wall, C. G.; Ou, W.; Erickson, B. W.; Bignozzi, C. A. *Inorg. Chem.* **1994**, *33*, 3952. (b) Carter, C.; Brumbach, M.; Donley, C.; Hreha, R. D.; Marder, S. R.; Domercq, B.; Yoo, S. H.; Kippelen, B.; Armstrong, N. R. *J. Phys. Chem. B* **2006**, *110*, 25191.

(16) Shukla, A. D.; Das, A.; van der Boom, M. E. *Angew. Chem., Int. Ed.* **2005**, *44*, 3237.

(17) (a) Remon, P.; Balter, M.; Li, S.; Andreasson, J.; Pischel, U. *J. Am. Chem. Soc.* **2011**, *131*, 20742. (b) de Ruiter, G.; van der Boom, M. E. *J. Mater. Chem.* **2011**, *21*, 17575. (c) Periyasamy, G.; Collin, J.-P.; Sauvage, J.-P.; Levine, R. D.; Remacle, F. *Chem.—Eur. J.* **2009**, *15*, 1310.

(18) Gupta, T.; van der Boom, M. E. *Angew. Chem., Int. Ed.* **2008**, *47*, 5322.

DOI: 10.1021/jacs.5b00586
J. Am. Chem. Soc. 2015, 137, 4058−4061